# *Ultrasonic Time of Flight Diffraction Defect Recognition based on Edge Detection*

Yuwen Cao, Haijiang Zhu
School of Information Science & Technology,
Beijing University of Chemical Technology,
Beijing, China.

Ping Yang
Acoustic Laboratory
National Institute of Metrology
Beijing, China.

*Abstract*—**We investigate a kind of method of ultrasonic time of flight diffraction defect recognition based on edge detection in this paper. Firstly, the ultrasonic B-scan image is accumulated by successive A-scan ultrasonic signals of defect on the specimen. Secondly, we choose one A-scan ultrasonic signal as the reference signal and calculate the cross correlation function between the reference signal and other A-scan ultrasonic signals. The B-scan image is calibrated by using the largest peak of each cross correlation function. Lastly, the B-scan image is denoised by Wiener filter, and edge detection operators are applied to the Wiener-denoised B-scan image and feature of defect are detected by using these operators. Thus defect can be recognized accurately from these feature detection results of B-scan ultrasonic image. Experimental results validate this method.**

***Keywords: defect recognition; ultrasonic TOFD image; Calibration; Edge detection operator.***

## I. INTRODUCTION

The time-of-flight-diffraction (TOFD) ultrasonic detection is a new method of non-destructive testing (NDT), which is based on measurement of the time of flight of the ultrasonic waves diffracted from the tips of defects, and has been widely used in defect recognition and size assessment. This technique first appeared in 1977 [1] and has a lot of advantages which make it the preferable technique in material testing. There are many successful examples for applying TOFD technique to give accurate size of defects and characterize of weld defects [2,3,4].

In recent years TOFD technique has been attracted more and more attention, and many new methods are combined with TOFD technique [5-10]. Gang Tie[5] presented a method of improving ultrasonic image resolution based on synthetic aperture focusing technique, thus lateral and vertical location of the crack tip can be measured rapidly and accurately by this method. Chi Dazhao[6,7] proposed crack tip recognition and weld defect detection by using image enhancement and energy distribution function of ultrasonic TOFD B-scan image. For data processing and interpretation of TOFD data required expert knowledge and accuracy largely depended on the operator experience, Shitole[8] presented a technique of automatic interpretation and classification of weld defects in TOFD data using three advanced methods including: an artificial neural network, a fuzzy logic and a hybrid neural-fuzzy. Using the Finite Difference Time Domain (FDTD) method, Satyanarayan[9] reported on the numerical simulations of the TOFD technique to image and size cracks in plate specimens. Zhang Yonghong[10] studied the TOFD technique for accurate crack size assessment by using the arrival time identification approach based on cross correlation.

In [6,7,9], Chi Dazhao dealt with some B-scan images and D-scan images of TOFD ultrasonic signal on weld defect. But the peak of the diffracted wave is far less than those of the lateral wave and the back wall echo, image of defect is not distinct in TOFD ultrasonic image. Therefore, it is difficult to recognize and assess clearly size of defect.

In our work, we investigate the calibration of ultrasonic TOFD B-scan image by estimating the cross correlation function between other A-scan signals and the reference signal, and apply image filter and edge detection operator to the B-scan image.

## II. B-SCAN IMAGE CALIBRATION ALGORITHM

### *A.Specimen and A-scan Signal*

The specimen is made of aluminum and its size is $250\times20\times480$ mm. There is a perforation at the 80mm distance far from the upper surface of the specimen. Ultrasonic TOFD detected system uses two probes, i.e. the transmitter and the receiver. The center frequency of probe is 2.5 MHz and the angle of probe is 45°. This detected system is shown in Fig. 1.

When ultrasound is introduced into the specimen, defect tip works as a point source of diffracted waves. The received signals can be visualized in an A-scan presentation as shown

978-1-4244-5316-0/10/$26.00 ©2010 IEEE

in Fig. 2(a), where X-axis represents the propagation time of the ultrasonic wave and Y-axis indicates the amplitude of the reflected wave. Because depth of this specimen is greater than the depth of the perforation and the back wall echo is very low, the back wall echo is omitted in sampling signal.

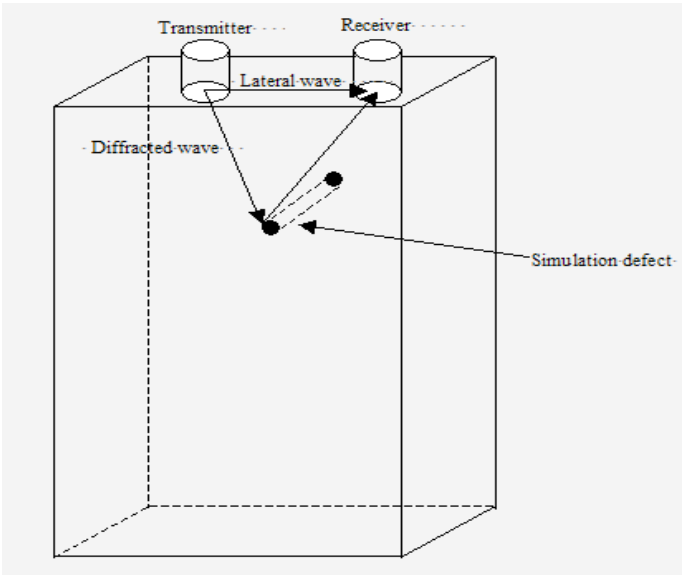


Fig.1. Specimen and TOFD technique

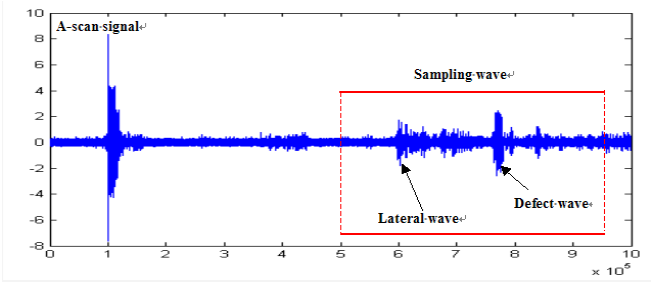


(a)

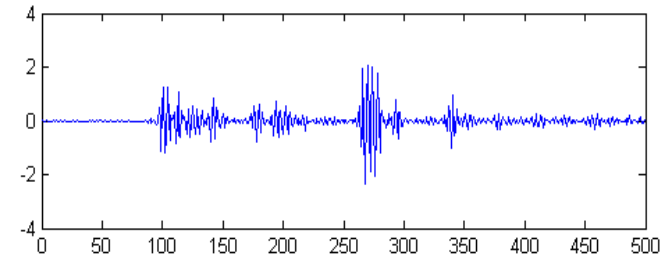

(b)

Fig.2. (a) original A-scan signal; (b) Sampling signals of A-scan signal from red rectangle in (a)

*B.B-scan Image Calibration Algorithm s*

Usually, a B-scan image is formed by an accumulation of successive A-scan ultrasonic signals, i.e. A-scan ultrasonic signals is represented by using digital image: gray value 0 is corresponding to a positive peak of A-scan signals, 255 is to a negative peak of A-scan signals and 128 is to a zero amplitude of A-scan signals.

In our experiment, ninety four A-scan signals are obtained and there are 500 sampling point in each A-scan signal. Thus, the B-scan image is shown as Fig. 3(a) and its size is $500\times94$ pixels. From this B-scan image, we can see that the lateral waves are sinuate and not on the line, and the defect echoes don't come into being smooth curves. Thus, the shape of defect is not easy to recognize. Therefore, the ultrasonic B-scan image must be calibrated in order to recognize accurately defect.

Suppose two A-scan signals are $x(t)$ and $y(t)$ respectively, their cross correlation function is the following:

$$R_{xy}(t)=\frac{1}{T}\int_0^T x(t)y(t+\tau)dt \tag{1}$$

Then the discrete description of $R_{xy}(t)$ is:

$$R_{xy}(\tau)=\frac{1}{n}\sum_{i=1}^{n}x(i)y(i+\tau) \tag{2}$$

Where $\tau$ is a delay interval between $x(t)$ and $y(t)$. From (2), the resulting peaks of the cross correlation function between $x(t)$ and $y(t)$ indicate the time of flight between these two signals. If we choose one A-scan signal as a reference signal $L_0$, and the delay intervals between other A-scan signals $L_n$ and the reference one can be calculated from (2). Ultrasonic B-scan image may be calibrated from these delay intervals between other A-scan signals and the reference one, the B-scan image calibration algorithm is as follow:

1. Acquire all A-scan signals and the number of A-scan signals.
2. Choose one A-scan signal as the reference signal $L_0$.
3. Calculate the cross correlation function $R_{xy}$ between other A-scan signals $L_n$ and the reference one $L_0$, and determinate the largest peak of $R_{xy}$ and the corresponding delay time interval $t$. Then find the medium value of all samplings in signals $L_n$ and $L_0$, and compute the difference between the delay time $t$ and the medium value of all samplings.
4. Shift the A-scan signal $L_n$ from the difference between the time $t$ and the medium value of all samplings and arrange other A-scan signals to the reference signal $L_0$, then save the shifted signals.
5. If $N\neq 0$, then go to step 3; otherwise go to step 6.
6. Accumulate of successive A-scan ultrasonic signals shifted in step 4, and the ultrasonic B-scan image is calibrated.

The calibrated B-scan image is acquired by applying B-scan image calibration algorithm, and Fig. 3(b) shows the calibrated B-scan image. From experimental results, we know that the lateral waves are almost horizontal lines and the defect echoes are some smooth curves with a few noises.

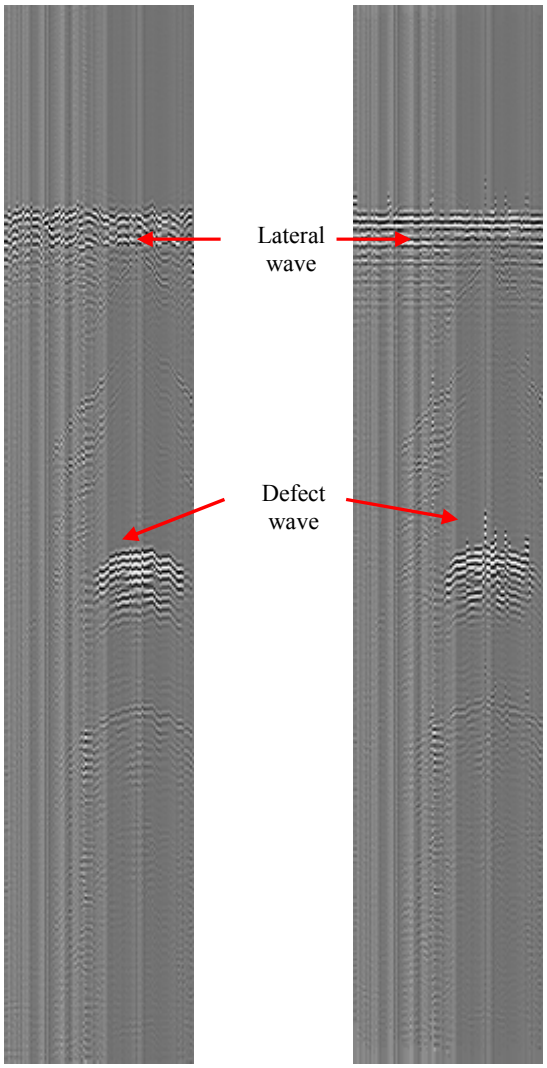


Fig.3. (a) Original B-scan image; (b) The calibrated B-scan image.

## III. IMAGE EDGE DETECTION

Edge is a kind of important feature information in image processing. Generally, there are many ways to perform edge detection. And the most may be grouped into two categories: edge detection method based on gradient and edge detection method based on zero-crossing feature. The gradient method detects the edges by looking for the maximum and minimum in the first derivative of the image. The second method searches for zero-crossings in the second derivative of the image to find edges. The gradient method includes Prewitt operator, Sobel operator, Canny operator and Roberts operator, and the zero-crossing feature method includes Log operator, Laplace operator and Gauss operator. In this section, we apply these edge detection operators to the B-scan image and obtain some distinct results.

In fact, only the echo of the defect is interesting in the B-scan image. Because the peak of the diffracted wave is far less than those of the lateral wave and the back wall echo, gray image of defect is not distinct in TOFD ultrasonic image. And it is difficult to recognize defect that there are noises in the B-scan image. Therefore, the B-scan image is first denoised by using Wiener filter; then image edge detection methods are used to the denoised B-scan image and edge feature of the lateral wave and the diffracted wave may be represented; last we can recognize easily the defect in the B-scan image. Fig. 4 shows some experimental results, where Fig. 4(a) is the Wiener-denoised B-scan image that is smoother than the calibrated B-scan image as shown in Fig. 3(b), Fig. 4(b), (c), (d), (e) are edge detection images by using Prewitt operators, Sobel operator, Roberts operator and Log operator respectively. From these edge detection images, we can see that edges of the lateral wave and the diffracted wave of defect are very distinct and the defect is easily recognized.

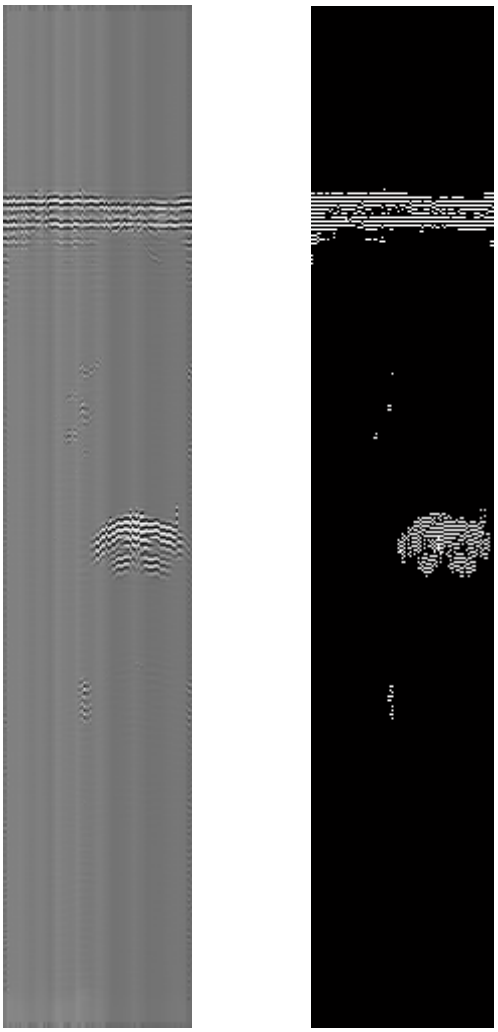

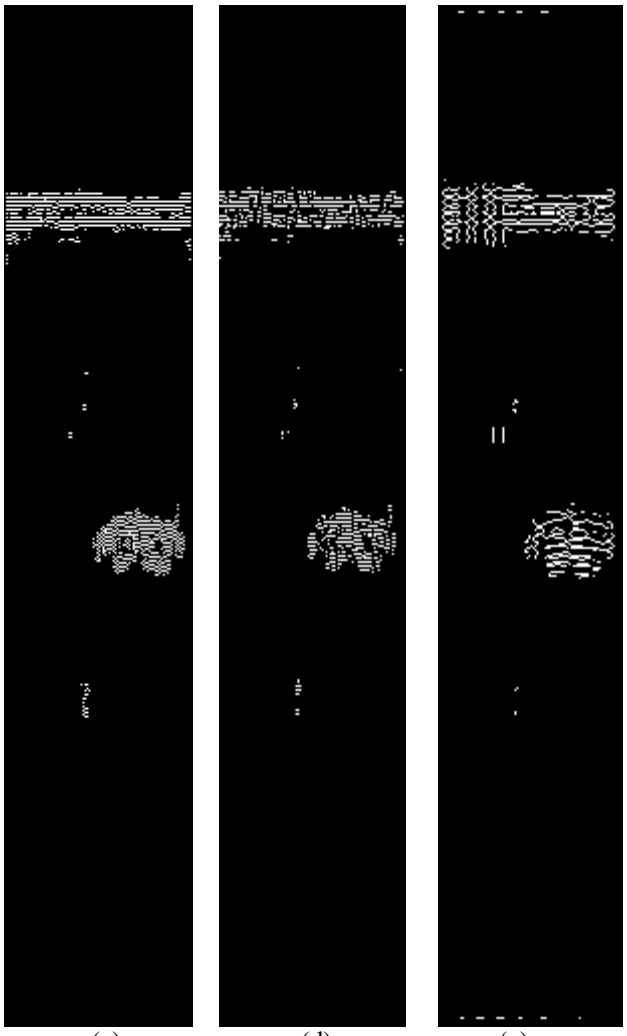

(c) (d) (e)

Fig.4. (a) Wiener-denoised B-scan image; (b) Prewitt-detected B-scan image; (c) Sobel-detected B-scan image;(d) Roberts-detected B-scan image; (e) Log-detected B-scan image.

## IV. CONCLUSION

In this work, we have presented an ultrasonic B-scan image calibration algorithm and edge detection of B-scan image. Here, the B-scan image is formed by an accumulation of successive A-scan ultrasonic signals; and through the cross correlation function between each two A-scan signals, the B-scan ultrasonic image is calibrated; after the B-scan image is denoised by Wiener filter, edge detection processing operators are used to the Wiener-denoised B-scan image, thus defect can be recognized accurately from these edge detection results of the B-scan ultrasonic image.

## ACKNOWLEDGMENT

We acknowledge the support provided by General Administration of Quality Supervision, Inspection and Quarantine of the People's Republic of China (No.AKY0709) and The Project Sponsored by the Scientific Research Foundation for the Returned Overseas Chinese Scholars, State Education Ministry.

## REFERENCES

[1] Silk M G. Sizing Crack-like Defects by Ultrasonic Means. Research Techniques in Non-destructive Testing[M]. London: London Academic Press, 1977.

[2] Trimborn N, The time-of-fight-diffraction technique, NDTnet, www.ndt.net/article/tofd /trimborn/ trimborn.htm, 1997,2(9)

[3] Krutzen R, Evaluation of currently applied ultrasonic sizing techniques for stress corrosion cracks in steam generator tubes, 17th EPRI Steam Generator NDE Workshop, Breckenridge,Colorado, USA, www. nuson. nl/ news/ do05 pres. html , Aug. 1998.

[4] Erhard A and Ewert U, The TOFD method between radiography and ultrasonic in weld testing, www.ndt.net/article /v04n09 /erhard / erhard.htm, 1999,4(9)

[5] Gang Tie, Chi Da-Zhao; Yuan Yuan. Ultrasonic TOFD technique and image enhancement based on synthetin aperture rousing technique. Hanjie Xuebao/Transactions of the China Welding, 2006,27(10):7-10 (Chinese)

[6] Chi Dazhao, Gang Tie; Sheng Zhaoyang. Method for crack tip recognition in an ultrasonic time of flight diffraction image. Chinese Journal of Mechanical Engineering, 2007,43(10):103-107 (Chinese).

[7] Chi Dazhao, Gang Tie, Gao Shuangsheng. Background removal and weld defect detection based on energy distribution of image. China Welding (English Edition), 2007,16(1):14-18

[8] Shitole C'S. N., Zahran O. , Al-Nuaimy W. Combining fuzzy logic and neural networks in classification of weld defects using ultrasonic time-of-flight diffraction. Insight: Non-Destructive Testing and Condition Monitoring, 2007,49(2): 79-82

[9] Satyanarayan L. Krishnamurthy C.V.; Balasubramaniam K. Finite difference time domain simulation of the time-of-flight diffraction technique for imaging and sizing cracks. Insight: Non-Destructive Testing and Condition Monitoring, 2007,49(12): 708-714

[10] Zhang Yonghong, Wang Yu; Zuo Ming J., Wang Xiaodong.Ultrasonic time-of-flight diffraction crack size identification based on cross-correlation. IEEE Canadian Conference on Electrical and Computer Engineering (CCECE), 2008:1797-1800.